Metal Dependence of the Highest Occupied Molecular Orbital in Sterically Hindered Octaethyltetraphenylporphyrins

Sharon A. Sibilia, Songzhou Hu, Christine Piffat,† Dan Melamed,‡ and Thomas G. Spiro*

Department of Chemistry, Princeton University, Princeton, New Jersey 08544

Received June 27, 1996[⊗]

Resonance Raman (RR) spectra are reported for nickel(II) and copper(II) 2,3,7,8,12,13,17,18-octaethyl-5,10,15,20-tetraphenylporphyrin (MOETPP) cation radicals in order to examine the influence of the substituent pattern and of out-of-plane distortions on the character of the porphyrin frontier orbitals. Isotopic frequency shifts ($^{13}C_m$, ^{15}N, d_{20}) were used to secure assignments of the RR bands. The highest occupied molecular orbital was found to switch from a_{2u} to a_{1u} between $CuOETPP^+$ and $NiOETPP^+$ as evidenced by (1) opposite shifts in the $C_\beta C_\beta$ stretching mode, ν_2, and (2) selective enhancement of phenyl modes in $CuOETPP^+$ vs ethyl modes in $NiOETPP^+$. However, the ν_2 shifts are smaller than those seen in $NiOEP^+$ (A_{1u}) or $CuTPP^+$ (A_{2u}), indicating that mixing of the A_{1u} and A_{2u} states is greater in the $OETPP^+$ radicals. A greater amount of mixing in $OETPP^+$ is consistent with a small energy gap between the two states and with the out-of-plane distortion. The dominant mixing mechanism is a bond alternant (A_{2g}) distortion, which is evident in the CuOETPP crystal structure and in the appearance of anomalously polarized bands in the Soret-enhanced radical cation RR spectra. Intensity analysis of the absorption spectra supports the inference of orbital switching between NiOETPP and CuOETPP but also indicates an increased energy gap between the two metals, relative to OEP and TPP. This increase in metal sensitivity is attributable to the out-of-plane distortions observed in Ni- and CuOETPP.

Introduction

Tetrapyrrolic π-cation radicals have been a focus for research, owing to their central role in the mechanism of the photosynthetic reaction center[1] and also of oxygen-activating heme proteins.[2] While peripheral substituents are known to influence the highest occupied molecular orbital (HOMO) of metalloporphyrins,[3,4] the role of out-of-plane distortions has recently come under scrutiny. Out-of-plane distortions have been observed in the crystal structures of the light-harvesting antenna bacteriochlorophyll *a* of *Prosthecochloris aestuarii*[5] and in the special pair bacteriochlorophylls *b* (BC-*b*) in the photosynthetic reaction center of *Rhodopseudomonas viridis*[6] (*Rps. viridis)*. Variations in the extent of the out-of-plane distortions, which are attributed to contacts with their protein environment, have been proposed as a possible reason for the directionality of electron transfer.[5−7] Several model compounds have been synthesized and characterized to facilitate the study of out-of-plane distortions.[8] These model porphyrins incorporate steric crowding of substituents, which leads to a saddling[9] distortion of the macrocycle, as is observed in metallo-2,3,7,8,12,13,17,18-octaethyl-5,10,15,20-tetraphenylporphyrins (MOETPPs) crystal structures.[10] The saddle distortion is greater for NiOETPP than for CuOETPP and persists in solution, according to variable temperature NMR data[10] which show high inversion barriers for the macrocycle.

However, the use of dodecasubstituted porphyrins as models for protein induced distortions is complicated by the electronic influence of the peripheral substituents themselves, which influence the ordering of the two highest occupied molecular orbitals (HOMOs), a_{1u} and a_{2u}.[11] Spellane et al. analyzed this issue some time ago,[4] using a semiempirical approach in which the intensity ratio of the Q bands, combined with their emission properties, was used to gauge the effects of substituents and of metal electronegativity on the frontier orbitals. Their conclusion was that $a_{1u} > a_{2u}$ for octaethylporphyrins (OEPs) but $a_{2u} > a_{1u}$

* Author to whom correspondence should be addressed.
† Present address: Department of Chemistry, University of Houston, Houston, TX 77004.
‡ Present address: Brookhaven National Laboratories, Upton, NY 11973.
⊗ Abstract published in *Advance ACS Abstracts,* February 1, 1997.

(1) (a) Bixon, M.; Fajer, J.; Feher, G.; Freed, J. H.; Gamliel, D.; Hoff, A. J.; Levanon, H.; Mobius, K.; Nechushtai, R.; Norris, J. R.; Scherz, A.; Sessler, J. L.; Stehlik, D. *Isr. J. Chem.* **1992**, *32*, 369. (b) Parson, W. W.; Ke, B. In *Photosynthesis: Energy Conversion by Plants and Bacteria*; Govindjee, Ed.; Academic Press: New York, 1982; Vol. I, Chapter 8.
(2) Dawson, J. H. *Science* **1988**, *240*, 433−439.
(3) (a) Czernuszewicz, R. S.; Macor, K. A.; Li, X. Y.; Kincaid, J. R.; Spiro, T. G. *J. Am. Chem. Soc.*, **1989**, *111*, 3860−3869. (b) Oertling, W. A.; Salehi, A.; Chang, C. K.; Babcock, G. T. *J. Phys. Chem.* **1989**, *93*, 1311−1319.
(4) Spellane, P. J.; Gouterman, M.; Antipas, A.; Kim, S.; Liu, Y. C. *Inorg. Chem.* **1980**, *19*, 386−391.
(5) Tronrud, D. E.; Schmid, M. F.; Matthews, B. W. *J. Mol. Biol*. **1986**, *188*, 443−454.
(6) Deisenhofer, J.; Michel, H. *Science* **1989**, *245*, 1463−1473.
(7) (a) Deisenhofer, J.; Michel, H. *Angew. Chem., Int. Ed. Engl.* **1989**, *28*, 829−847. (b) Alden, R. G.; Ondrias, M. R.; Shelnutt, J. A. *J. Am. Chem. Soc.* **1990**, *112*, 691−697. (c) Furenlid, L. R.; Renner, M. W.; Smith, K. M.; Fajer, J. *J. Am. Chem. Soc.* **1990**, *112*, 1634−1635. (d) Furenlid, L. R.; Renner, M. W.; Fajer, J. *J. Am. Chem. Soc.* **1990**, *112*, 8987−8989. (e) Geno, M. K.; Halpern, J. *J. Am. Chem. Soc.* **1987**, *109*, 1238−1240.
(8) (a) Barkigia, L. M.; Chantranupong, L.; Smith, K. M.; Fajer, J. *J. Am. Chem. Soc.* **1988**, *110*, 7566−7567. (b) Gudowska-Nowak, E.; Newton, M.; Fajer, J. *J. Phys. Chem.* **1990**, *94*, 5795−5801.
(9) Nomenclature defined by: Scheidt, W. R.; Lee, Y. *J. Struct. Bonding* **1987**, *64*, 1−70. The saddle distortion consists of displacement of alternate pyrrole rings above and below the mean plane of the porphyrin defined by the 24 core atoms.
(10) (a) Shelnutt, J. A.; Medforth, C. J.; Berber, M. D.; Barkigia, K. M.; Smith, K. M. *J. Am. Chem. Soc.* **1991**, *113*, 4077−4087. (b) Medforth, C. J.; Senge, M. O.; Smith, K. M.; Sparks, L. D.; Shelnutt, J. A. *J. Am. Chem. Soc.* **1992**, *114*, 9859−9869. (c) Barkigia, K. M.; Renner, M. W.; Furenlid, L. R.; Medforth, C. J.; Smith, K. M.; Fajer, J. *J. Am. Chem. Soc.* **1993**, *115*, 3627−3635. (d) Barkigia, K. M.; Berber, M. D.; Fajer, J.; Medforth, C. J.; Renner, M. W.; Smith, K. M. *J. Am. Chem. Soc.* **1990**, *112*, 8851−8857. (e) Medforth, C. J.; Berber, M. D.; Smith, K. M.; Shelnutt, J. A. *Tetrahedron Lett.* **1990**, *31*, 3719−3722.
(11) Gouterman, M. In *The Porphyrins*; Dolphin, D., Ed.; Academic Press: New York, 1978; Vol. III, Chapter 1.

S0020-1669(96)00774-4 CCC: $14.00

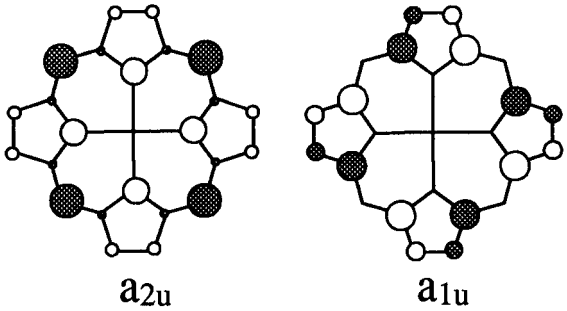

Figure 1. A_{1u} and A_{2u} orbital patterns The sizes of the circles are proportional to the atomic orbital (AO) coefficients of magnesium porphine. The black and white circles represent positive and negative signs, respectively, of the upper lobes of the p_π orbitals.[3,11]

for tetraphenylporphyrins (TPPs). This inference was later confirmed by resonance Raman (RR) studies[3] of the radical cations which showed that the frequency shifts are consistent with a_{1u} character for all $MOEP^+$s but with a_{2u} character for all TPP^+s. The orbitals are expected to be close in energy when both ethyl and phenyl substituents are present. Recent calculations[12] predict that the influence of C_m-tetraphenyl substitution dominates over C_β-octaethyl substitution in MOETPPs, since electron density at the meso carbons in a_{2u} is much larger than at the β-pyrrole carbons in either orbital (Figure 1). Support for this prediction is found in the triplet state of ZnOETPP, which shows an a_{2u} time resolved EPR signal[13] and from the FTIR marker band shift[14] of $CuOETPP^+$. Likewise, the absence of an ESR signal in the $CuOETPP^+$ radical[14] is attributed to antiferromagnetic spin coupling of the metal and a_{2u} cation spins. However, the influence of the metal on the orbital ordering has not been investigated.

In this study, we present the RR spectra of the π-cation radicals of NiOETPP and CuOETPP. Resonance Raman spectroscopy is a useful probe of metalloporphyrin electronic structure, since the vibrational frequency shifts reflect changes in bond order when an electron is removed from the π-framework. We find that the shift of the prominent ν_2 marker band upon formation of the cation changes direction from $CuOETPP^+$ to $NiOETPP^+$. This marker band, primarily a $C_\beta C_\beta$ stretch, is an established[3] probe of the HOMO, since the $C_\beta C_\beta$ bonding pattern is opposite for the a_{2u} and a_{1u} orbitals. However, alternation of adjacent $C_\alpha C_m$ bond lengths in the $CuOETPP^+$ radical crystal structure,[14] in the absence of intermolecular contacts, is indicative of mixing of the A_{1u} and A_{2u} states along an A_{2g} distortion. The small $MOETPP^+$ skeletal mode frequency shifts, relative to $MOEP^+$ and $MTPP^+$, and the appearance of anomalously polarized (ap) A_{2g} modes in the Soret-enhanced spectra of the cations point to A_{1u}/A_{2u} mixing in the $MOETPP^+$ radicals via a pseudo-Jahn−Teller effect, which is augmented by the out-of-plane distortion.

Experimental Section

Octaethyltetraphenylporphyrin was synthesized by condensation of benzaldehyde and 3,4-diethylpyrrole[10d] and purified by column chromatography on alumina. Ni(II) and Cu(II) were incorporated using the dimethylformamide (DMF) procedure[15] and purified on a silica plate.

The first and second oxidation potentials of the porphyrins were measured by cyclic voltammetry (CV) in CH_2Cl_2 using 0.001 M porphyrin and 0.1 M tetrabutylammonium hexafluorophosphate ($TBA(PF_6)$) or tetrabutylammonium perchlorate (TBAP) as supporting electrolyte. The CVs were obtained in a three compartment cell, fit with gas inlets to purge the solution and to flow Ar over the working electrode compartment. A platinum disk working electrode was separated by fine and medium porosity disks from the saturated sodium chloride (SSCE) reference and platinum wire counter electrodes. Potentials were obtained with a BAS CV27 potentiostat and the results plotted on a Houston Instruments 100 $X-Y$ recorder. Ferrocene was used as a standard.

The absorption spectrum of $NiOETPP^+$ was obtained by chemical oxidation of NiOETPP with $AgClO_4$ in methylene chloride and by bulk electrolysis (0.1 M TBAP in CH_2Cl_2) in a 2 cm path length spectroelectrochemistry cell fit with a platinum gauze working electrode, a platinum counter electrode, and an SSCE reference electrode. A PAR 173 potentiostat with a PAR 175 programmer was used for bulk electrolysis. Oxidation by both methods resulted in the same UV/vis spectrum. CuOETPP was chemically oxidized with $AgClO_4$ in order to obtain the absorption spectrum. Data were collected on either a HP 8451A (bulk electrolysis) or a HP 8452A (chemical oxidation) UV/vis spectrometer. The NiOETPP and CuOETPP cation radicals for the RR measurements were generated electrochemically in a bulk electrolysis cell similar to the one described by Czernuszewicz and Macor[16] with 0.1 M $TBA(PF_6)$ (NiOETPP and isotopomers) or TBAP (NiOETPP, CuOETPP) as supporting electrolyte. The NiOETPP RR data did not change upon changing the supporting electrolyte from $TBA(PF_6)$ to TBAP.

The excitation wavelengths were 406.7 and 413.1 nm for RR spectra, generated with a Coherent Nova 400 Kr^+ ion laser, and 457.9 nm, generated with a Spectra Physics 2001 Ar^+ ion laser. The scattered light was dispersed by a Spex 1401 monochromator and detected by a cooled RCA 31034A photomultiplier tube. Laser powers of 50−100 mW at the sample were used, and a spectral resolution of 4 cm^{-1} was typical. The neutral species scans were collected at 1 cm^{-1} steps for 1 s integration times. The cation radical spectra were the sum of two scans taken under the same conditions as the spectra of the neutral species, since scattering from the cations was much weaker. Reversibility was checked for each sample by reducing the oxidized species to obtain the neutral species RR spectrum again. All measurements were obtained at room temperature.

Absorption spectra for the Q band analysis were obtained on a HP 8452A UV/vis spectrometer, using the neat solvent as background. The absorbance ratios were obtained by measuring the ratio of the Q_0 and Q_1 peak areas.

Results

A. Electrochemistry and UV/Vis Spectra. As in the case of NiTPP,[17,18] the CV of NiOETPP is sensitive to the solvent and electrolyte. In methylene chloride reversible waves were observed for the first oxidation, at 0.63 and 0.54 V vs SSCE in 0.1 M TBAP and 0.1 M $TBA(PF_6)$, respectively. Both potentials are lower than the previously reported value of 0.85 V vs SCE in butyronitrile.[10c] A similar dependence of the oxidation potential of CuOETPP on solvent and electrolyte was recently reported.[14] We observed its first oxidation potential at 0.37 V vs SSCE in methylene chloride containing 0.1 M TBAP. As previously noted,[10c] the MOETPP oxidation potentials are much lower than the oxidation potential of the corresponding TPPs and OEPs. For example NiTPP is oxidized at 1.05 V (TBAP) or 1.01 V ($TBA(PF_6)$) vs SCE in CH_2Cl_2,[19] and CuTPP is oxidized at 0.90 V (TBAP or TPrAP) vs SCE in

(12) Skillman A. G.; Collins, J. R.; Loew, G. H. *J. Am. Chem. Soc.* **1992**, *114*, 9538−9544.
(13) Regev, A.; Galili, T.; Medforth, C. J.; Smith, K. M.; Barkigia, K. M.; Fajer, J.; Levanon, H. *J. Phys. Chem.* **1994**, *98*, 2520−2526.
(14) Renner, M. W.; Barkigia, K. M.; Zhang, Y.; Medforth, C. J.; Smith, K. M.; Fajer, J. *J. Am. Chem. Soc.* **1994**, *116*, 8582−8592.
(15) Buchler, J. W. In *Porphyrins and Metalloporphyrins*; Smith, K. M., Ed.; Elsevier: Amsterdam, 1975; Chapter 5.
(16) Czernuszewicz, R. S.; Macor, K. A. *J. Raman Spectrosc.* **1988**, *19*, 553−557.
(17) Kadish, K. M.; Van Caemelbecke, E.; Boulas, P.; D'Souza, F.; Vogel, E.; Kisters, M.; Medforth, C. J.; Smith, K. M. *Inorg. Chem.* **1993**, *32*, 4177−4178.
(18) Godziela, G. M.; Goff, J. M. *J. Am. Chem. Soc.* **1986**, *108*, 2237−2243.
(19) Chang, D.; Malinski, T.; Ulman, A.; Kadish, K. M. *Inorg. Chem.* **1984**, *23*, 817−824.

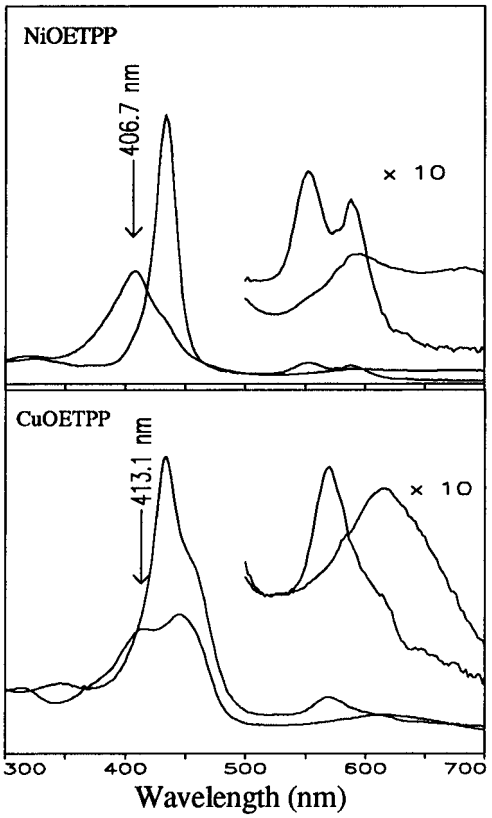

Figure 2. Absorption spectra of (a) NiOETPP (- -) and NiOETPP$^+$ (—) and (b) CuOETPP (- -) and CuOETPP$^+$ (—). The cations were prepared by chemical oxidation with $Ag(ClO_4)$ in CH_2Cl_2. The Q band region is shown with 10-fold amplification. Identical spectra were obtained electrochemically for both porphyrins (see text). Arrows indicate the excitation wavelengths for RR spectroscopy.

Table 1. UV/Vis Spectra and Electrochemical Oxidation Potentials[a] of NiOETPP and CuOETPP and Their Cation Radicals

		$E_{1/2,ox1}$		$E_{1/2,ox2}$	
	Wavelength (nm)	TBAP	$TBAPF_6$	TBAP	$TBAPF_6$
NiOETPP	442, 552, 558	0.63	0.54	0.90	0.90
NiOETPP$^+$	408, 592, 682				
CuOETPP	433 (460)sh, 570, 654	0.37	—	0.96	—
CuOETPP$^+$	414 (446)sh, 618, 764				

[a] Potentials (V) measured in methylene chloride with a Pt disk working electrode and Pt wire counter electrode vs SSCE. The electrolyte concentration was 0.1 M, and the porphyrin concentration was 1×10^{-3} M for all experiments.

CH_2Cl_2.[20] More facile oxidation of the porphyrin macrocycle is typical of the sterically hindered porphyrins and is indicative of HOMO destabilization.

While the absorption spectrum of neutral NiOETPP (Figure 2a) contains a sharp Soret band, the CuOETPP absorption spectrum (Figure 2b) shows a 460 nm shoulder to the 433 nm Soret band. This shoulder, which has also been observed in butyronitrile,[14] does not arise from free base or chlorin.[21] As in CuTPP, the Q_0 band intensity of CuOETPP is very low both in the neutral species and in the cation, whereas the NiOETPP Q_0 band is quite intense. Oxidation of NiOETPP and CuOETPP resulted in green solutions, the absorption spectra of which showed blue shifted Soret and red shifted Q bands (Table 1), which are characteristic of porphyrin centered oxidation.[22]

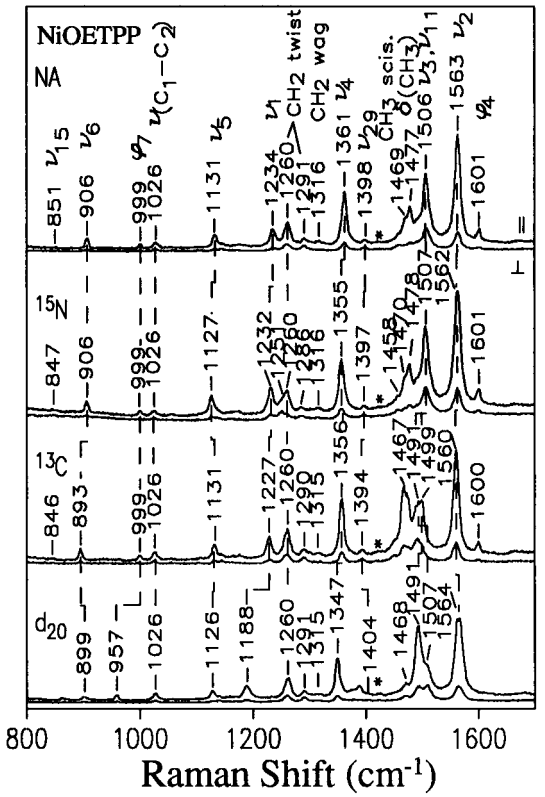

Figure 3. 406.7 nm excited RR spectra of NiOETPP, including the natural abundance (NA) and the pyrrole nitrogen (^{15}N), meso carbon (^{13}C), and perdeuterophenyl (d_{20}) isotopomers. These spectra were recorded in parallel (∥) and perpendicular (⊥) polarization.

B. RR Spectra of NiOETPP and Its Cation. Neutral Species. The RR spectra of natural abundance (NA) NiOETPP along with its nitrogen-15 (^{15}N), meso carbon-13 (^{13}C), and perdeuterophenyl (d_{20}) isotopomers are presented in Figure 3. The bands are labeled according to previous assignments,[23] and dashed lines correlate corresponding modes in the isotopic spectra. The excitation wavelength (406.7 nm) was chosen to coincide with the Soret maximum of NiOETPP$^+$ in order to minimize interference from any residual neutral species in the cation spectra (Figure 4). The 406.7 nm excited neutral NiOETPP spectra show the same enhancement pattern as the previously reported 441.6 nm-excited spectra.[24] The ^{15}N spectrum of NiOETPP has not been previously published.

The strongest bands arise from A_{1g} modes, as is expected for A-term scattering.[25] Substituent modes such as the CH_2 scissors, CH_2 twist and wag, C_1-C_2 stretch, and phenyl modes (ϕ_4, ϕ_5, and ϕ_7) are also enhanced. The band at 1506 cm^{-1} contains overlapping contributions from ν_3 and ν_{11}. Since ν_3 and ν_{11} have different isotopic sensitivities,[23,24] the two modes split in the ^{13}C and d_{20} spectra.

Cation. The RR spectra of natural abundance (NA) NiOETPP$^+$ along with its nitrogen-15 (^{15}N), meso carbon-13 (^{13}C), and phenyl deuterium (d_{20}) isotopomers are presented in Figure 4. Assignments of the cation modes are made from polarization measurements, from isotopic frequency shifts and by reference to MOEP and MTPP radical cation spectra.[3] The mode

(20) (a) Felton, R. H. *The Porphyrins*; Dolphin, D., Ed.; Academic Press: New York, 1978; Vol. 5, p 53. (b) Davis, D. G. In *The Porphyrins*; Dolphin, D., Ed.; Academic Press: New York, 1978; Vol. 5, p 127.
(21) Evans, B.; Smith, K. M. *Tetrahedron Lett.* **1977**, *5*, 443−446.
(22) Wolberg, A.; Manassen, J. *J. Am. Chem. Soc.* **1970**, *92*, 2982−2991.
(23) (a) Li, X.-Y.; Czernuszewicz, R. S.; Kincaid, J. R.; Us, Y. O.; Spiro, T. G. *J. Phys. Chem.* **1990**, *94*, 31−46. (b) Li, X.-Y.; Czernuszewicz, R. S.; Kincaid, J. R.; Stein, P.; Spiro, T. G., *J. Phys. Chem.* **1990**, *94*, 31−47.
(24) Piffat, C. A.; Melamed, D., Spiro, T. G. *J. Phys. Chem.* **1993**, *97*, 7441−7450.
(25) Johnson, B. B.; Peticolas, W. L. *Annu. Rev. Phys. Chem.* **1976**, *27*, 465−491.

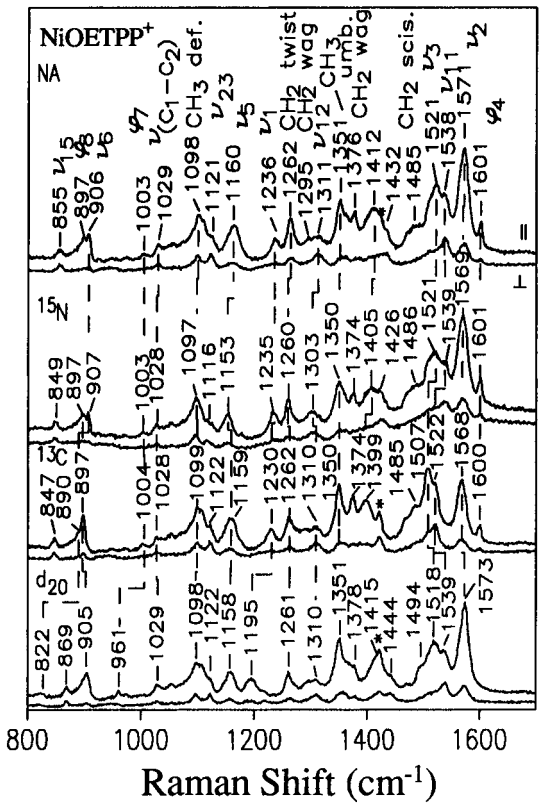

Figure 4. As in Figure 3 for NiOETPP$^+$, formed electrochemically in methylene chloride with 0.1 M TBA(PF_6) as supporting electrolyte.

assignments and isotopic frequency shifts are summarized in Table 2 and compared with those of the neutral molecule, and with selected isotopomers of CuTPP, CuTPP$^+$, NiOEP, and NiOEP$^+$. Marked shifts upon cation formation are seen for ν_2, ν_3, and ν_{11}. The isotope-insensitive polarized bands in the 1300−1400 cm^{-1} region are assigned to ethyl modes. Their frequencies agree with ethyl modes calculated for NiOETPP and observed in the neutral species spectra at different excitations.[24] The ν_4 skeletal mode is also expected in this region, but the large number of ethyl modes make identification difficult. One candidate is the 1412 cm^{-1} band which has the expected isotopic frequency changes, but a 51 cm^{-1} upshift from its position in NiOETPP seems excessive. The isotopic frequency shifts of the cation RR bands are similar to those of the neutral molecule, except that ν_3 shows a much lower d_{20} shift (3 cm^{-1} vs 15 cm^{-1}) and a larger $^{13}C_m$ shift (14 cm^{-1} vs 7 cm^{-1}) in the cation. These changes imply an altered mode composition, possibly reflecting a conformation change upon cation formation.

An anomalously polarized band at 940 cm^{-1} (Figure 5) probably arises from a greatly perturbed A_{2g} mode resulting from a pseudo-Jahn−Teller effect, as discussed for MOEP and MTPP radical cations.[3]

C. RR Spectra of CuOETPP and its Cation. Resonance Raman spectra of CuOETPP, enhanced with 413.1 nm excitation, are presented in Figure 6. The bands are assigned from polarization measurements, from $^{13}C_m$ isotopic frequency changes, and by comparison with NiOETPP[24] and the parent compounds, CuOEP and CuTPP.[3] They are in general accord with those previously suggested.[26] The 413.1 nm excitation wavelength was chosen to maximize the signal from the cation. As in NiOETPP, the 1503 cm^{-1} band has contributions from ν_3 and ν_{11}, which separate in the $^{13}C_m$ spectrum. Substituent modes are enhanced at 413.1 nm, as are several non-totally-symmetric skeletal modes.

The CuOETPP$^+$ spectra (Figure 6) were assigned via polarization measurements, via $^{13}C_m$ isotopic frequency shifts, and by comparison with NiOETPP$^+$, CuOEP$^+$, and CuTPP$^+$. The frequencies of the $^{13}C_m$ isotopomer (shown in parentheses in Table 2) indicate that the normal mode eigenvectors are very similar for the neutral and cation CuOETPP. Small shifts are observed for the majority of the skeletal modes in CuOETPP$^+$ relative to the neutral species. The ν_{11} band shifts up strongly, however, from 1503 to 1524 cm^{-1}. It is again difficult to assign the ν_4 frequency due to the number of ethyl modes enhanced in the 1300−1400 cm^{-1} region. Two ap modes are seen at 869 and 972 cm^{-1} (Figure 5), which both downshift upon $^{13}C_m$ substitution to 861 and 963 cm^{-1}, respectively.

Discussion

Orbital Ordering Changes Observed. Two pieces of evidence lead us to conclude that the relative order of the a_{1u} and a_{2u} orbitals are reversed in Cu- and NiOETPP: marker bands shift in opposite direction upon oxidation, and opposite enhancements are observed for phenyl vs ethyl modes. In other metalloporphyrins,[3] radical cation formation produces an upshift in the prominent ν_2 marker band when the HOMO is a_{1u} and a downshift when the HOMO is a_{2u}. These shifts are consistent with the orbital patterns (Figure 1), which are bonding (a_{2u}) and antibonding (a_{1u}) with respect to the $C_\beta C_\beta$ bonds, whose stretching coordinates are the main contributions to ν_2. The ν_2 downshift (−4 cm^{-1}) for CuOETPP$^+$ therefore supports an a_{2u} HOMO, while the upshift (8 cm^{-1}) of ν_2 in NiOETPP$^+$ supports an a_{1u} HOMO. The ν_2 isotope shifts (Table 2) are invariant between NiOETPP and NiOETPP$^+$ and also between CuOETPP and CuOETPP$^+$, eliminating the possibility that oxidation might change the eigenvector. Recent INDO/CI calculations for a series of dodecasubstituted nickel porphyrins[26] predicted a_{1u} to be higher than a_{2u} in NiOETPP.

Additional evidence for orbital switching comes from the enhancement of substituent modes in the cation radical spectra. In CuOETPP$^+$, the enhancement of the phenyl mode, ϕ_4, is much stronger, relative to the skeletal modes, than in the neutral species; it is actually the strongest band in the spectrum (Figure 6). An increase in ϕ_4 intensity was likewise observed in CuTPP$^+$ [3] but might have resulted from borrowed intensity because of the near coincidence of the phenyl mode (1595 cm^{-1}) with ν_{10} (1586 cm^{-1}). In CuOETPP$^+$, the frequencies are farther apart (1597 cm^{-1} for ϕ_4 and 1563 cm^{-1} for neutral ν_{10}), making intensity borrowing unlikely. In contrast, ϕ_4 is not strongly enhanced for NiOETPP$^+$, but ethyl modes (e.g., CH_3 modes at 1098 and 1351 cm^{-1}, CH_2 modes at 1262 and 1376 cm^{-1}) are much stronger, relative to the skeletal modes, than in the neutral species.

Substituent mode intensity changes in the radicals may be explained by delocalization of the electron hole onto the substituent. In EPR spectra of metalloporphyrin cations, delocalization of spin density is observed on the β carbons for A_{1u} and on the C_m carbons for A_{2u} radicals.[27] Additional delocalization onto the attached substituents can lead to RR enhancement of the substituent modes.[28] Structural evidence for delocalization of electron density from phenyl substituents is seen in the crystal structure of CuOETPP$^+$, for which the

(26) Sparks, L. D.; Medforth, C. J.; Park, M.-S.; Chamberlain, J. R.; Ondrias, M. R.; Senge, M. O.; Smith, K. M.; Shelnutt, J. A. *J. Am. Chem. Soc.* **1993**, *115*, 581−592.

(27) Fajer, J.; Davis, M. S. *The Porphyrins*; Dolphin, D., Ed.; Academic Press: New York, 1979; Vol. IV, Chapter 4.

(28) Renner, M. W.; Cheng, R.-J.; Chang, C. K.; Fajer, J. *J. Phys. Chem.* **1990**, *94*, 8508−8511.

Table 2. Resonance Raman Frequencies (cm^{-1}) and Isotope Shifts[a]

	NiOETPP[b]/+		CuOETPP/+		CuTPP/+ [c]		NiOEP/+ [c]		NiTPP[d]
mode	NA(^{15}N,^{13}C,d_{20})	NA(^{15}N,^{13}C,d_{20})	NA(^{13}C)	NA(^{13}C)	NA(d_{20})	NA(d_{20})	NA(^{15}N)	NA(^{15}N)	NA(^{15}N,^{13}C,d_{20})
ν_2	1563 (−1,−3,1)	1571 (−2,−3,2)	1557 (−3)	1553 (−2)	1562 (−4)	1578 (−4)	1600 (0)	1623 (0)	1572 (0,−8,4)
ν_3	1506 (1,−7,−15)	1521 (0,−14,−3)	1503 (−7)	1499 (−4)	–	–	–	–	1470 (0,−6,8)
ν_{11}	1506 (1,−15,1)	1538 (1,−16,1)	1503 (−15)	1524 (−13)	1501 (0)	1496 (−5)	1575 (0)	1608 (0)	1504 (0,0,0)
ν_4	1361 (−6,−5,−14)	–	1356 (−3)	–	1365 (5)	1355 (9)	1383 (7)	1368 (10)	1374 (−6,9,−11)
ν_1	1234 (−2,−7,−46)	1236 (−1,−6,−41)	1238 (−7)	1236 (−6)	1237 (−51)	1234 (−45)	–	–	1235 (−1,−16,−50)
ν_5	1131 (−4,0,−5)	1160 (−7,−1,−2)	1130 (0)	–	–	–	1138 (6)	1140 (5)	–
ap[e]		940 (−7,−2,−3)		972 (−9)		959		958 (−7)	
ν_6	906 (0,−13,−7)	906 (1,−16,−1)	905 (−11)	899 (−9)	1008 (11)	1002 (7)	–	–	1004 (−20,−2,−6)
ap				869 (−8)		899			
ϕ_4	1601 (0,−1,−)	1601 (0,−1,−)	1598 (0)	1597 (0)	1599 (−48)	1599 (−34)	–	–	1599 (−,−,0)
ϕ_7	999 (0,0,−42)	1003 (0,1,−42)	1001 (0)	999 (−1)	–	–	–	–	

[a] Observed frequencies in CH_2Cl_2/0.1 M TBA(PF_6) solution with 406.7 nm excitation. NA = natural abundance, d_{20} = ^{2}H substituted analogues at phenyl carbon positions, ^{13}C = meso ^{13}C substitution, and ^{15}N = pyrrole ^{15}N substitution. [b] Assignments from Piffat et al.[24] [c] Data from Czernuszewicz et al.[3] [d] Data from Li et al.[23] [e] ap = anomalously polarized.

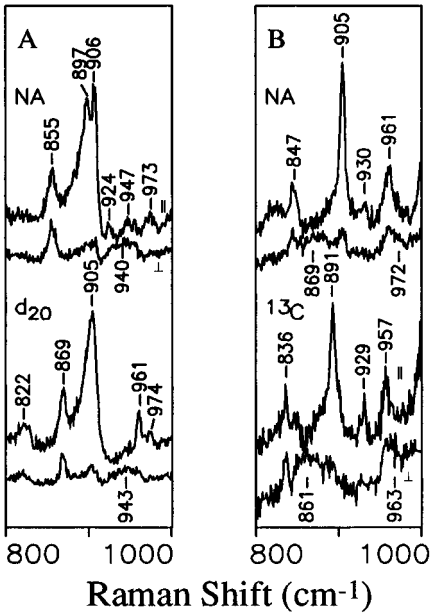

Figure 5. Enlargement of the mid-frequency region of the (A) NiOETPP cation (406.7 nm excitation) and (B) CuOETPP cation (457.9 nm excitation), showing anomalously polarized bands (greater intensity in perpendicular (⊥) than in parallel (∥) polarization).

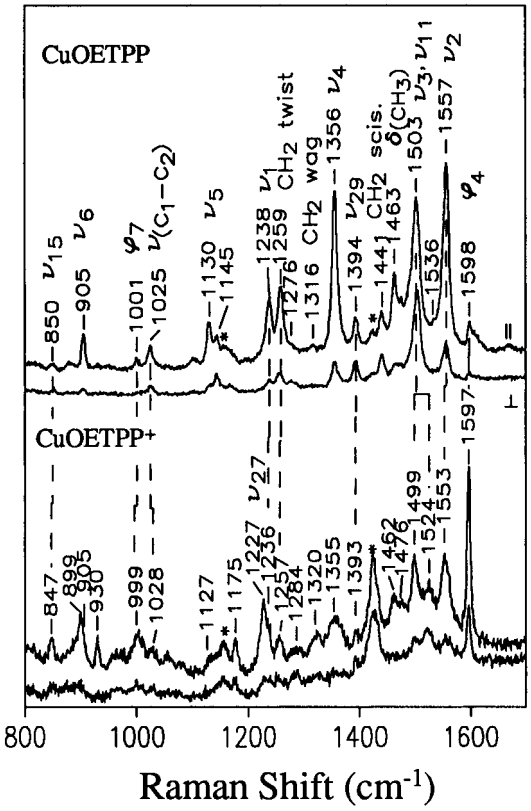

Figure 6. 413.1 nm excited RR spectra of CuOETPP and CuOETPP$^+$ formed electrochemically in methylene chloride with 0.1 M TBAP as supporting electrolyte. Parallel (∥) and perpendicular (⊥) polarizations are shown.

porphyrin−phenyl dihedral angle is smaller (average 33°) than in the neutral species (average 45.6°). Thus, the substituent enhancement pattern supports A_{2u} character for CuOETPP$^+$ and A_{1u} character for NiOETPP$^+$.

Mixing Mechanisms. The ν_2 shifts in the MOETPPs (−4 and +8 cm^{-1}) are small compared to NiOEP (+23 cm^{-1}) and CuTPP (−32 cm^{-1}).[3] This diminution is evidence for orbital mixing in the radicals. Although the a_{1u} and a_{2u} HOMOs are orthogonal in D_{4h} symmetry, they can be mixed via a pseudo-Jahn−Teller (pJT) effect. Evidence for such mixing was provided by the observation of anomalously polarized A_{2g} (A_{2g} = $A_{1u} \times A_{2u}$) modes in the RR spectra of MOEP$^+$ and MTPP$^+$ radicals at frequencies much lower than the A_{2g} modes of the neutral porphyrins.[3] Such modes are also seen in the MOETPP$^+$ spectra (940 cm^{-1} for NiOETPP$^+$, 869 and 972 cm^{-1} for CuOETPP$^+$). These bands are quite weak in the MOETPP$^+$ spectra, probably because the modes lose A_{2g} character as a result of the out-of-plane distortions, which lower the molecular symmetry from D_{4h}.

It is reasonable that the mixing would be greater for the MOETPP$^+$ than the MOEP$^+$ or MTPP$^+$ radicals, because the a_{1u} and a_{2u} are closer in energy, the HOMO switching from one to the other when Ni is replaced by Cu. This mechanism has also been invoked by Jayaraj et al.[29] and by Barzilay et al.[30] to explain small ν_2 shifts in (oxoferryl) and in manganese and zinc porphyrin π-cations, respectively, when meso-aryl substituents contain electron withdrawing groups that bring the a_{1u} and a_{2u} orbitals close in energy. In addition to the pJT effect, orbital mixing can be induced in the OETPP$^+$ radicals by the S_4 out-of-plane distortion (a_{1u}, $a_{2u} \rightarrow$ b).[31]

Other evidence for orbital mixing comes from the observation of bond alternation, an A_{2g} symmetry distortion. A MNDO-level calculation[32] of the zinc porphine excited state geometry

(29) Jayaraj, K.; Terner, J.; Gold, A.; Roberts, D. A.; Austin, R. N.; Mandon, D.; Weiss, R.; Bill, E.; Müther, M.; Trautwein, A. X. *Inorg. Chem.* **1996**, *35*, 1632−1640.
(30) Barzilay, C. M.; Sibilia, S. A.; Spiro, T. G.; Gross, Z. *Chem. Eur. J.* **1995**, *1*, 222−231.
(31) Lin, C.-Y.; Hu, S.; Rush, T.; Spiro, T. G. Submitted for publication.
(32) Prendergast, K.; Spiro, T. G., *J. Phys. Chem.* **1991**, *95*, 9728−9736.

Table 3. Shifts in Resonance Raman Frequencies (cm^{-1}) upon Formation of Cation Radicals: Comparison of $NiOETPP^+$ and $CuOETPP^+$ with $NiOEP^+$, $NiTPP^+$, $CuOEP^+$, and $CuTPP^+$[a]

mode	$NiOETPP^+$[b]	Δ[c]	$NiOEP^+$	Δ	$NiTPP^+$	Δ	$CuOETPP^+$[d]	Δ	$CuOEP^+$	Δ	$CuTPP^+$	
ν_2	1571	8	1623	23	1532	−38	1553	−4	1613	21	1530	−32
ν_{11}	1538	32	1608	33			1524	21	1601	33	1496	−5
ν_3	1521	15	1511	−8			1499	−4	1498	−4		
ν_1	1236	2			1236	−2	1236	−2			1237	−3
ν_5	1160	29	1138	2					1136	0		

[a] Data on the frequencies and cationic shifts of NiOEP, NiTPP, CuOEP, and CuTPP are from Czernuszewicz et al.[3] [b] Observed frequencies in CH_2Cl_2 (0.1 M TBA(PF_6)) with 406.7 nm excitation. [c] Δ = frequency shifts upon formation of the cation radical ($\nu_{cation} - \nu_{neutral}$). [d] Observed frequencies in CH_2Cl_2 (0.1 M TBAP) with 413.1 nm excitation.

predicts substantial alternation of the bonds around the 16-membered inner ring, as a result of a_{1u}/a_{2u} orbital mixing. Bond alternation is apparent in the crystal structures of $ZnOEP^+$ [33] and $CuOETPP^+$.[14] For $ZnOEP^+$, Scheidt and co-workers[33] attributed the distortion to close intermolecular contacts within pairs of molecules. But $CuOETPP^+$ molecules are prevented by the bulky substituents from approaching each other closely.[14] The bond alternation in this structure is a clear demonstration of orbital mixing.

As a result of this mixing, the orbital coefficients are altered.[32] The bonding/antibonding dichotomy is diminished for the $C_\beta C_\beta$ bonds, thereby accounting for the diminished ν_2 shifts in the $MOETPP^+$ radicals. Also, the HOMO becomes alternatingly bonding and antibonding for the $C_\alpha C_m$ bonds, consistent with the bond distance alternation in the radicals. This pattern might account for an interesting discrepancy between the frequency shifts of ν_2 and ν_{11}. Like ν_2, ν_{11} has been found to be a marker of orbital character, shifting up for $MOEP^+$ radicals and down for $MTPP^+$ radicals.[3] However, ν_{11} shifts up for both $NiOETPP^+$ and $CuOETPP^+$ (Table 2). In addition to $C_\beta C_\beta$ stretching, ν_{11} has an important contribution from the out-of-phase combination of adjacent $C_\alpha C_m$ stretches. The force constant for this coordinate may be selectively increased when an electron is removed from an orbital having alternating bonding and antibonding character for adjacent $C_\alpha C_m$ bonds. Thus, increased orbital mixing could also account for the lack of parallelism between ν_2 and ν_{11} in the $OETPP^+$ radicals.

Factors Controlling the Orbital Energies. Spellane et al. analyzed the $a_{1u}-a_{2u}$ energy gap via an intensity analysis[4] based on the absorption spectra and emission properties of several metalloporphyrins. The Soret (B) and Q_0 transitions are formed by configuration interaction between the two excitations, $a_{1u} \rightarrow e_g$ and $a_{2u} \rightarrow e_g$, in the four orbital model.[11] When the a_{1u} and a_{2u} orbitals are equal in energy, the Q_0 intensity should fall to zero due to destructive interactions of the transition moments. The other band in the Q region, Q_1, is attributed to vibronic coupling between the two states. Since Q_1 intensity is relatively constant,[34] the Q_0/Q_1 ratio serves as a measure of the relative energy difference between the two orbitals, by the formula

$$A\{Q_{(0,0)}\}/A\{Q_{(1,0)}\} = \text{constant}[^1E(a_{1u}e_g) - {}^1E(a_{2u}e_g)]^2$$

Applying this formula to data for TPPs, OEPs, and porphines (P), Spellane et al. constructed the HOMO energy diagram shown in Figure 7, which we have augmented by calculating the energies for the OETPPs and also NiOEP and NiTPP (Table 4).[35] The a_{1u}/a_{2u} energy crossover ($\Delta E = 0$) is expected to lie higher on the diagram for triplet states than for singlet states

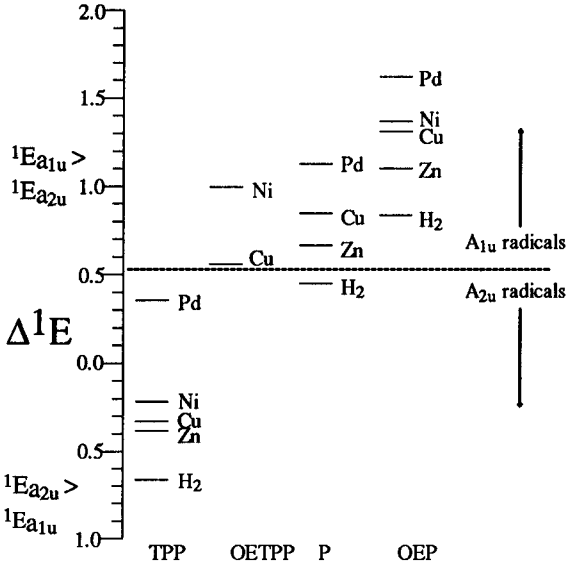

Figure 7. Absorption intensity-derived energy differences between the a_{1u} and a_{2u} orbitals in the indicated metalloporphyrins (P = porphine) according to Spellane et al.[4] The entries for the OETPPs and for NiTPP and NiOEP are from the present work. The dashed line (- -) represents the approximate offset between the neutral singlet state $\Delta E = 0$ and the cation radical $\Delta E = 0$ to account for exchange and Coulombic interactions between electron and hole orbitals (0.326 eV) (see text).

Table 4. Ratio of Absorbance Peaks [$Q_{(0,0)}/Q_{(1,0)}$][a]

	TPP	OETPP	P	OEP
H_2	0.43		0.17	0.78
Zn	0.13		0.44	1.35
Cu	0.095	0.33[b]	0.76	1.75
Ni	0.088[b]	0.98[b]		2.32[b]
Pd	0.11		1.37	2.70

[a] Data from Spellane et al.[4] unless otherwise marked. [b] This work.

due to the differing $a_{1u}-a_{2u}$ exchange integral. The same $\Delta E = 0$ is expected for cation radicals as for triplets, on the assumption that the electron−hole interaction integrals, as well as the solvation energies, cancel in the cation.[4] Porphyrins lying above the $\Delta E = 0$ line are expected to have an a_{1u} HOMO, while those below the line are expected to have an a_{2u} HOMO.

The OETPPs fall at positions intermediate between the OEPs and the TPPs, as expected from electronic substituent arguments. Competing destabilization of the a_{2u} and a_{1u} orbitals by the C_m-phenyl and C_β-alkyl substituents[36] places the MOETPP orbital energy gaps near those of porphine. Meso-substituents perturb

(33) Song, H.; Reed, C. A.; Scheidt, W. R. *J. Am. Chem. Soc.* **1989**, *111*, 6867−6868.
(34) Perrin, M. H.; Gouterman M.; Perrin, C. L. *J. Chem. Phys.* **1969**, *50*, 4137−4150.
(35) We note that Binstead et. al. (Binstead, R. A.; Crossley, M. J.; Hush, N. S. *Inorg. Chem.* **1991**, *30*, 1259−1264) have developed a method for estimating the a_{1u}/a_{2u} energy differences which has fewer assumptions but which relies on porphyrin oxidation and reduction potentials as well as the absorption energies, data which are incomplete for the molecules included in Figure 4.
(36) Gouterman, M. *J. Chem. Phys.* **1959**, *30*, 1139−1161.

the a_{2u} orbital, which has large coefficients of electron density at C_m, but not the a_{1u} orbital since it has nodes at C_m. Substituents at C_β, however, perturb a_{1u} more than a_{2u} because of larger electron density coefficients at C_β in the a_{1u} orbital. These effects are borne out by earlier reports, including EPR,[37] FTIR,[38] and RR[3] data, which confirm that the electron is abstracted from the a_{2u} orbital in MTPPs and from the a_{1u} orbital in MOEPs. The intermediate position of the OETPPs on the diagram is consistent with the observation of orbital switching when Cu replaces Ni. Although this result suggests that the $\Delta E = 0$ should lie above CuOETPP$^+$, rather than slightly below it, the discrepancy is well within the uncertainties in the intensity analysis.[4]

The order of the different metals in Figure 7 is the order of their electronegativities.[4] The metal ion interacts selectively with the a_{2u} orbital, which is concentrated at the pyrrole N atoms, whereas the N atoms are at nodes in the a_{1u} orbital. The greater the electronegativity of the metal, the greater the stabilization of the a_{2u} orbital via the positive charge of the metal. This accounts for Ni lying higher than Cu for all of the porphyrins.

However, the calculated energy gap between Ni and Cu is much larger for OETPP (0.65 eV) than for TPP (0.012 eV) or OEP (0.20 eV). The larger gap is attributed to the saddling distortion which is experienced by all OETPPs as a result of the steric clash of the substituents, but is greater for NiOETPP than for CuOETPP due to the shorter Ni−N(pyrrole) bonds.[26] The distortion destabilizes the HOMO (now a mixture of a_{1u} and a_{2u} orbitals)[31] because of misalignment of the π-system. Thus, the NiOETPP HOMO is raised relative to the CuOETPP HOMO. An additional factor is that the out-of-plane distortion allows the HOMO (which has electron density at the N atoms as a result of its a_{2u} character) to interact with the $d_{x^2-y^2}$ orbital of the metal. This interaction should be more stabilizing for Ni^{2+} than Cu^{2+} because the $d_{x^2-y^2}$ orbital is empty for Ni^{2+} but half-filled for Cu^{2+}. Again, the effect is to increase ΔE for Ni relative to Cu. A similar effect on the porphyrin HOMO is observed in the Ni- and CuOETPP oxidation potential difference (0.26 V) vs Ni- and CuTPP (0.15 V), showing that the MOETPP out-of-plane distortion increases the sensitivity of the porphyrin ring to the metal.

Conclusions

The RR data presented in this study confirm that CuOETPP$^+$ is an A_{2u} cation and identify the NiOETPP$^+$ cation as A_{1u} on the basis of ν_2 marker band shifts and selective increases in substituent mode enhancements. The MOETPP a_{1u} and a_{2u} orbitals are found to be closer in energy than they are in MOEPs or MTPPs, reflecting competing electronic effects of the peripheral substituents. However, a larger change in the orbital energies when Ni is replaced by Cu is observed in the MOETPPs than in the MOEPs or MTPPs. This large change in the orbital energies is attributed to the sterically-induced out-of-plane distortion in the MOETPPs and to distortion-induced orbital interactions, both of which are larger for Ni than for Cu.

In both NiOETPP$^+$ and CuOETPP$^+$, the orbitals are mixed by a pseudo-Jahn−Teller distortion, which is reinforced by the sterically-induced distortion, as evidenced by (1) small ν_2 shifts due to reduced $C_\beta C_\beta$ bonding and antibonding interactions in the mixed orbitals, (2) strong upshifts of ν_{11} in both cations, reflecting augmentation of the asymmetric $C_\alpha C_m$ stretching force constant as a result of bond alternation (evidenced in the CuOETPP$^+$ crystal structure), and (3) the appearance of anomalously polarized modes in the Soret-enhanced spectra.

In heme enzyme catalytic systems, deviations of the porphyrin ring induced by its surroundings may influence the energy and electron density characteristics of the porphyrin ring orbitals, as well as their interactions with the central metal ion. In synthetic catalytic systems, both electronic substituent effects and sterically induced out-of-plane distortions will be important in determining the porphyrin−metal interactions.

Acknowledgment. The authors thank Dr. Jack Fajer for helpful discussions. This research was supported by NIH Grant GM 33576.

IC960774+

(37) Fajer, J.; Borg, D. C.; Forman, A.; Felton, R. H.; Vegh, L.; Dolphin, D. *Ann. N.Y. Acad. Sci. 1973, 206*, 177−199.
(38) Hu, S.; Spiro, T. G. *J. Am. Chem. Soc.* **1993**, *115*, 12029−12034.